Optical Materials: X 27 (2025) 100425

Contents lists available at ScienceDirect

Optical Materials: X

journal homepage: www.journals.elsevier.com/optical-materials-x

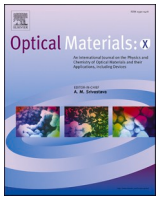

Design and preparation of water soluble NIR emitters based on isocyanide pincer Pt(II) complexes copolymerized with polyvinylpyrrolidon

Elizaveta V. Durova [a], Rostislav R. Shulepov [a], Vadim A. Baigildin [a], Mikhail A. Kinzhalov [a], Mikhail P. Kurlykin [b], Viktor V. Sokolov [a], Sergey P. Tunik [a,*]

[a] Saint-Petersburg State University, 7/9 Universitetskaya Nab., St. Petersburg, 199034, the Russian Federation
[b] Saint-Petersburg State University of Industrial Technologies and Design, 18 Bolshaya Morskaya ul., Saint-Petersburg, 191186, the Russian Federation

A B S T R A C T

A series of Pt(II) NˆNˆC pincer complexes bearing isocyanide-styrene ligand in the fourth position was synthesized and their photophysics was studied in detail. In solution the complexes exhibit phosphorescence from ^{3}MLCT excited state, whereas in solid state due to crystal packing effects all but one complexes display ^{3}MMLCT emission accompanied by a considerable red shift of emission band, which may be ascribed to formation of binary aggregates with short Pt–Pt contacts. The styrene function of the isocyanide ligand allows complexes copolymerizing with polyvinylpyrrolidone *via* RAFT chemistry to give amphiphilic block copolymers with the hydrophobic block consisting of a few "back-to-back" copolymerized platinum complexes. In organic solvent, the copolymers exist as isolated molecular entities showing a limited intramolecular aggregation of the platinum chromophores analogous to their behavior in the solid state. On the contrary, in aqueous media hydrophobicity of the platinum containing blocks provokes formation of micellar type nanospecies, demonstrating intermolecular aggregation of the platinum chromophores with tighter contacts of the platinum centers and multiple character of the aggregates. This behavior results in much stronger red shift of emission into NIR area that makes the copolymers promising for application in biological experiments as NIR emitting probes.

1. Introduction

Square planar Pt(II) complexes containing isocyanide ligands attract considerable attention due to unusual reactivity patterns [1,2], catalytic activity in diverse organic transformations [3] and excellent photophysical properties [4–7], which make them promising for photonic applications [8–10]. Among wide variety of luminescent isocyanide complexes those based on pincer-type ligands (e.g. NˆNˆC, NˆNˆN, NˆCˆN) with an isocyanide moiety in the fourth position are of particular interest because of high emission quantum yield, easily tunable absorption and luminescent spectra and ability to afford aggregates, which demonstrate aggregation induced emission (AIE) due to the π−π interaction between aromatic systems of pincer ligands and metallophilic Pt–Pt bonding. The latter way of intermolecular interactions results in transformation of MLCT character of singlet and triplet excited states typical for mononuclear Pt(II) chromophores into MMLCT to give a considerable red shift of absorption and emission bands, which may appear in NIR region. The AIE phenomena demonstrated by the complexes of the $[(N^{\wedge}N^{\wedge}C)Pt(CNR)]^+$ type have been extensively studied in a large series of publications from Professor Che group [11–15] and some other research teams [16–18]. It has been shown that these mononuclear complexes display a clearly detectable trend to afford aggregates even in organic solution taking part in equilibria between monomeric and dimeric forms of the molecules [11,12], the position of the equilibrium is determined by steric properties of the pincer and isocyanide ligands. It is worth noting that careful selection of aggregation conditions, media pH and complexes' counterions can afford various superstructures, e. g. nanowires [12,19], nanorods and nanofibers [14], and mesophases [13,20]. Dependence of aggregation degree on pH made possible to use the corresponding complexes for estimation of pH in biological systems, e.g. for identification of acidic character of some cell compartments, especially in cancer cell lines [14].

Because the forces responsible for the aggregation are relatively weak obtaining of stable aggregates usually depends on additional support of the interaction between mononuclear chromophores, that can be provided, for example, by the bridging ligands [11,16,18] or by packing of the complexes in crystal cells of macro- and nanocrystals [11,12]. As for the application of AIEgens of this type in biological studies, it is highly desirable to render these chromophores water-soluble and stable in aqueous media. In the present communication we report on the synthesis of four [Pt(II)(NˆNˆC)L] pincer complexes, containing isocyanide ligand (L) functionalized by styrene group. The presence of styrene function made possible to use the complexes in RAFT polymerization reaction with polyvinylpyrrolidon to eventually obtain

* Corresponding author.
E-mail address: sergey.tunik@spbu.ru (S.P. Tunik).

https://doi.org/10.1016/j.omx.2025.100425
Received 11 August 2025; Received in revised form 27 September 2025; Accepted 17 October 2025
Available online 27 November 2025

amphiphilic block copolymers containing the hydrophobic fragments, which are able to form intermolecular aggregates in aqueous media demonstrating AIE behavior of platinum chromophores. The photophysical characteristics of the complexes in organic solutions, solid state and block copolymers in organic and aqueous media were studied and discussed from the viewpoint of their intra- and intermolecular aggregation.

2. Results and discussion

A series of five Pt(II) isocyanide complexes bearing various NˆNˆC pincer ligands were synthesized via the three-step reaction sequence shown in Scheme 1.

Following recrystallization the target compounds were obtained as crystalline solids, which however did not give single crystals suitable for X-ray diffraction study. Therefore, their characterization was performed by using HR ESI^+ mass spectrometry and NMR spectroscopy. Mass spectra of the complexes (Figs. S1–S5) display dominating signal of molecular ions with the isotopic patterns, which fit completely the stoichiometry of the molecule shown in Scheme 1. The ^1H NMR spectra (Figs. S6–S12) feature clearly distinguishable signals of the NˆNˆC and isocyanide ligands, the number of which, their multiplicity and relative intensity are completely compatible with the general structural pattern shown above. It is worth stressing that styrene double bond resonances remain in the spectra that indicate potential applicability of the obtained compounds for polymerization chemistry, *vide infra*.

The obtained complexes luminesce in dichloromethane (DCM) solution and in solid state with the quantum yield (QY) up to 13.6 % in degassed DCM, see Table 1 and Figs. 1 and 2. In solution the emission of the complexes display strong Stokes shift, lifetimes in microsecond domain and effective quenching with oxygen that clearly point to its origin from excited triplet state, i.e. phosphorescence. It is worth noting that emission band profiles and positions of the band maxima are not changing upon variations in the energy of excitation (300, 350, 400 nm), which points on the unique emissive excited state operative for each of these chromophores.

In our recent paper [21], the closely analogous platinum pincer complexes containing a different isocyanide ligand (2,6-dimethylphenyl isocyanide) have been studied experimentally and theoretically. The photophysical data obtained in DCM in the present study are essentially similar to those revealed earlier for the analogous chromophores that point to negligible participation of the isocyanide ligand in formation of emissive excited state and make possible to assign the nature of the lowest energy (LE) transitions in the absorption spectra and that of emissive excited state to the mixed ^{3}ILCT/^{3}MLCT [dπ{C/Pt} → π*{NN}] character as it has been done in the previous publication [21]. Absorption spectra of the complexes display strong bands that correspond to the intraligand (^{1}LC) π→ π* transitions located in a relatively narrow interval of 280–290 nm. The LE bands for the complexes containing C-coordinated phenyl moiety with different substituents similarly do not exhibit significant variations in the position of the band maxima, which fall in the range 341–351 nm that does not allow making meaningful correlation with the donor properties of the substituents. However, increase in the size of C-coordinated aromatic system in **Pt–BTh** gives immediate red shift of the LE band, which fits well strong contribution of the ^{3}MLCT character into this transition. On the contrary, the positions of emission band maxima for the complexes containing CF_3 – Cl – Me – OMe substituents in C-coordinated aromatic fragment correlate well (see Table 1 and Fig. 1) with the donor/acceptor character of the substituents in metalated fragment of the pincer ligand, which takes part in formation of emissive excited state as an electron donor; the stronger electron withdrawing substituents the higher energy (shorter wavelength) of emissive transition. Similar to the absorption spectra, emission band of the **Pt–BTh** complex is strongly red shifted to the NIR region evidently due to major contribution of ^{3}MLCT component and lower energy of benzothiophene π* orbitals compared to those of phenyl moiety in the other complexes. Emission bands of the **Pt-CF3** and **Pt–Cl** complexes containing electron withdrawing substituents display vibronic progression with spacing between the components' of ca. 1200–1300 nm that fit well vibrational frequencies of aromatic systems in the pincer ligand. This observation indicates that in these chromophores the contribution of the electron transition inside the coordinated ligand plays the major role, whereas in the other complexes ^{3}MLCT character determines the nature of the observed emission to give featureless emission bands.

Emission characteristics of the chromophores in solid state are essentially different from those in DCM solution due to well-known trend [21–25] of the platinum complexes of this type to aggregate in solid phase. Indeed, all but one (**Pt–BTh**) complexes display substantial red shift of emission bands ranging from 40 nm (**Pt–OMe**) to 175 nm (**Pt–Me**) compared to the data obtained in solution. The observed red shift may be ascribed to the Pt–Pt interaction and admixture/domination of ^{3}MMLCT character in the emissive excited state of the aggregated chromophores. The value of the shift is evidently determined by the efficacy of metallophilic bonding in the aggregates, which in turn is dictated by mutual orientation of the individual platinum chromophores participating in aggregation and by the number complexes forming the aggregate [21]. Unfortunately we were unable to elucidate packing patterns of the complexes in crystal cells, but the above conclusion is supported by crystallographic and photophysical data obtained earlier for essentially similar platinum isocyanide complexes [21]. A small blue emission shift in the solid state for **Pt–BTh** may be explained by

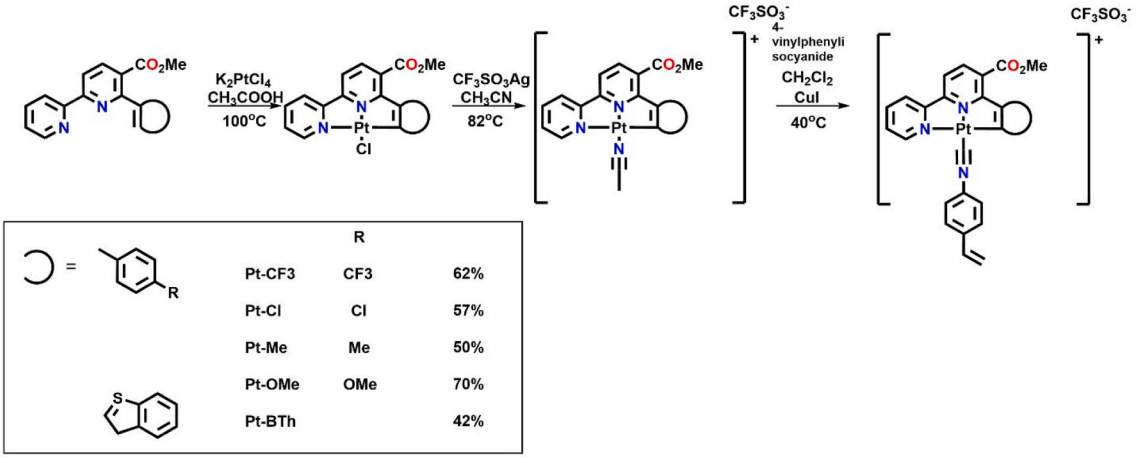

Scheme 1. Synthesis of **Pt–CF3** – **Pt–BTh** complexes.

Table 1
Photophysical characteristics of **Pt–CF3 – Pt–BTh** complexes in DCM solution (10^{-5} M) and solid state at 298K. Emission decays were monitored at the maximum of λ_{em} and treated with monoexponential analysis.

Compound	Solutions in CH_2Cl_2					Solid state			
	λ_{abs}, nm	λ_{exc}, nm	λ_{em}[a], nm	$\Phi_{aer/deg}$[b], %	$\tau_{aer/deg}$[b], ns	λ_{exc}, nm	λ_{em}[a], nm	Φ, %	τ, ns
Pt-CF3	274, 335sh, 351, 420sh	354, 418sh	520, 555, 605	3.6/8.9	1226/1726	440sh, 484	640	0.10	769
Pt–Cl	277, 341, 421sh	252, 325, 402sh	532, 569sh	4.2/13.6	2201/4432	519sh	700	4.39	520
Pt–Me	274, 346, 435sh	359, 462	548	4.0/5.7	448/670	384, 408sh	720	0.01	546
Pt–OMe	279, 348, 435sh	279, 352, 439	615	3.2/8.6	460/958	485sh	655	0.19	90
Pt–BTh	278, 360sh, 399, 499sh	500, 706, 823	720	1.6/3.6	158/294	397	705	0.01	113

[a] λ_{exc} = 365 nm.
[b] aer/deg – aerated and degassed solutions, respectively.

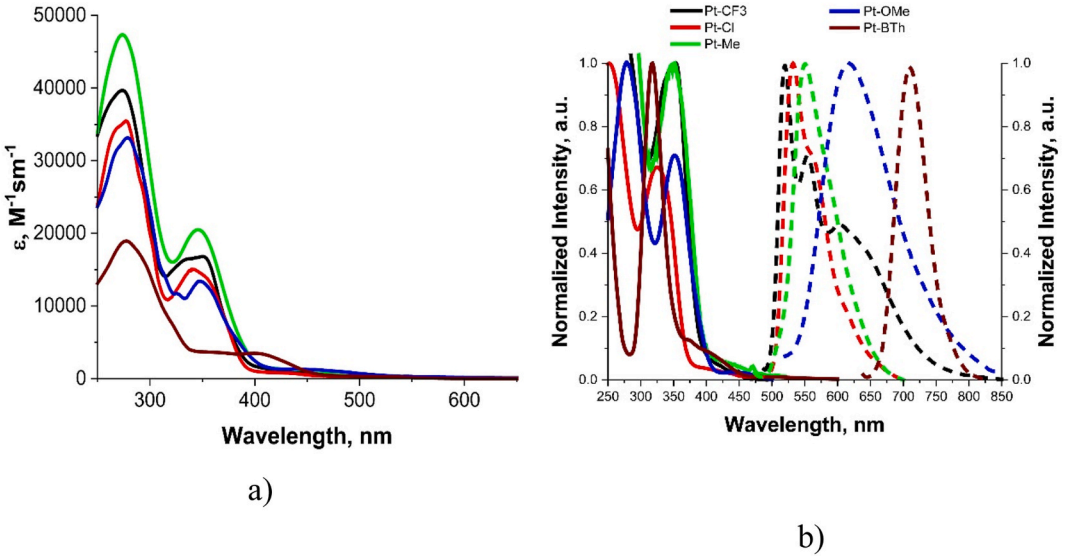

Fig. 1. a - Absorption spectra of **Pt–CF3** – **Pt–BTh**, b – normalized excitation (left) and emission (right) spectra of **Pt–CF3** – **Pt–BTh** solutions in DCM at concentration 10^{-5} mol/L, 298K.

extremely unfavorable packing of the complex in crystal cell, which prevents Pt–Pt contacts, whereas the variations in emission energy may be caused by π–π interaction of the pincer ligand aromatic systems in the cell. In accord with the EnergyGapLaw [26,27] the shift of emission band to NIR area results in effective vibrational quenching of emission to give substantially lower quantum yields and shorter excited state lifetimes. We cannot also exclude additional channel of excited state deactivation due to stacking of pincer ligands aromatic systems and formation of dark excimers, especially in the case of **Pt–BTh**.

The presence of styrene function in isocyanide ligand allows polymerizing the complexes with polyvinylpyrrolidone, which acts as macro-RAFT agent, to afford amphiphilic block copolymers, see Scheme 2. This approach was successfully applied several times [25,28,29] to obtain water soluble and biocompatible chromophores with emission fit the biological window of transparency.

The copolymers were characterized using gel-permission chromatography (GPC), dynamic light scattering (DLS), Transmission Electron Microscopy (TEM), and Inductively Coupled Plasma Optical Emission Spectroscopy (ICP OES). The obtained characteristics are summarized in Table 2 and Figs. S13 and S14. The main feature of obtaining the block copolymers with Pt complexes containing a polymerizable function is a stepwise manner realized by the triple addition of the initiator to the reaction mixture every 2 days, which allows the step by step bonding of the chromophore to the polymer chain. However, in contrast to the reaction carried out earlier [25,28,29] the copolymerization of Pt complexes with isocyanide-styrene ligand has led to the loss of products solubility and formation of a dispersion even at the second day of reaction. Apparently, the growing Pt-# blocks brought insolubility of the product in acetonitrile that resulted in the formation of precipitate and did not allow full consumption of the complex in polymerization process. Such a behavior when the chain-extension proceeds and the growing copolymer eventually becomes insoluble is an example of polymerization-induced self-assembly (PISA) [30]. It is worth noting that final copolymers obtained by PISA can be copolymerized only to some critical degree of polymerization due to insolubility of the products and can afford nanospecies with different morphologies depending on the second block length [31–34] thus leaving some amount of starting compounds unreacted including **p(VP)**. The procedure used for isolation of block copolymers (dialysis of water soluble reaction mixture components for 2 days, MWCO (molecular weight cut-off) ≥ 3500) removed unreacted platinum complex but did not allow separation of unreacted **p(VP)** from the copolymers due to the similarity of their molecular weights. This means that such characteristics as molecular weight and amount of Pt units per copolymer obtained by using GPC and ICP OES (Table 2 and S1) are in fact the magnitudes representing the corresponding parameter averaged across the ensemble, which also includes unreacted **p(VP)**. This is why, for example, the average number of platinum units in some copolymers is less than 1.0. Nevertheless, the photophysical data clearly indicate, *vide infra*, that dominating part of the copolymers' molecules contain at least two platinum units in the hydrophobic blocks.

It was found that the copolymers exist in organic solution (DCM) in the form of individual molecules, whereas in aqueous phase due to their amphiphilic character they form nanoparticles (NPS) most probably of micellar type [25,28,29].

The diameters of the NPS measured by DLS do not exceed 75 nm for

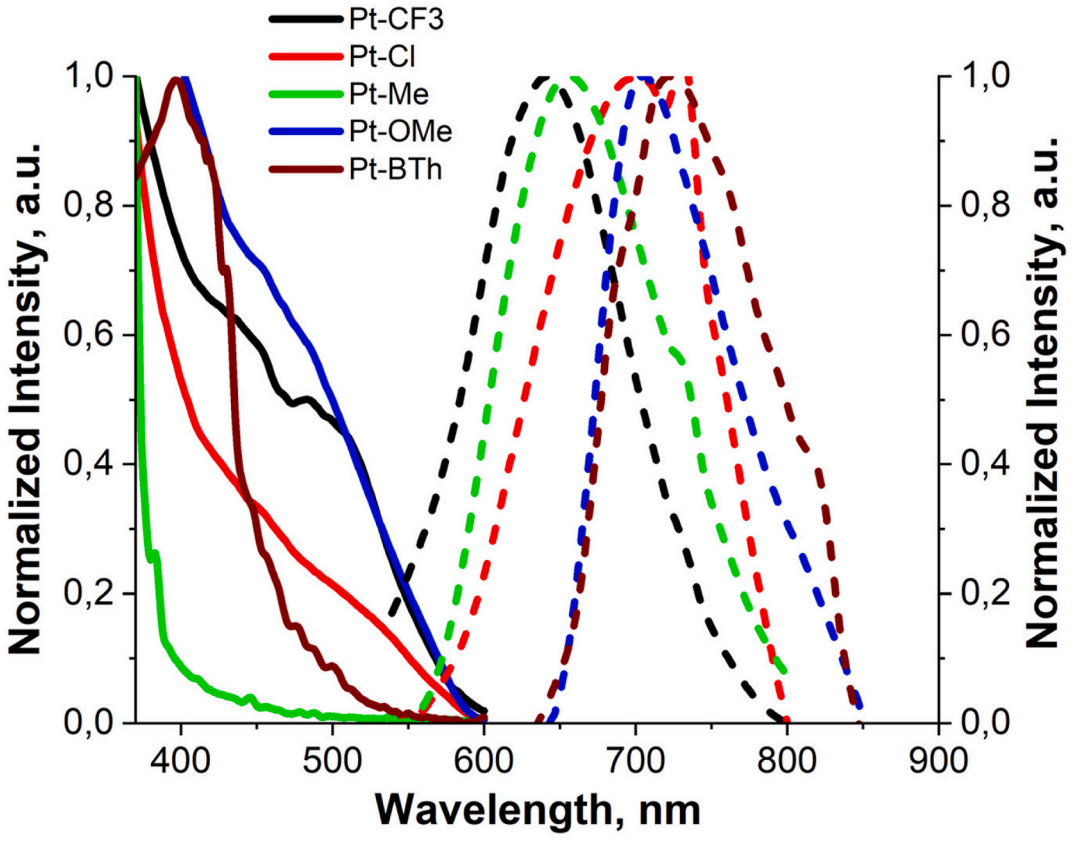

Fig. 2. Excitation (left) and emission (right) spectra of the **Pt–CF3** – **Pt–BTh** complexes in solid state.

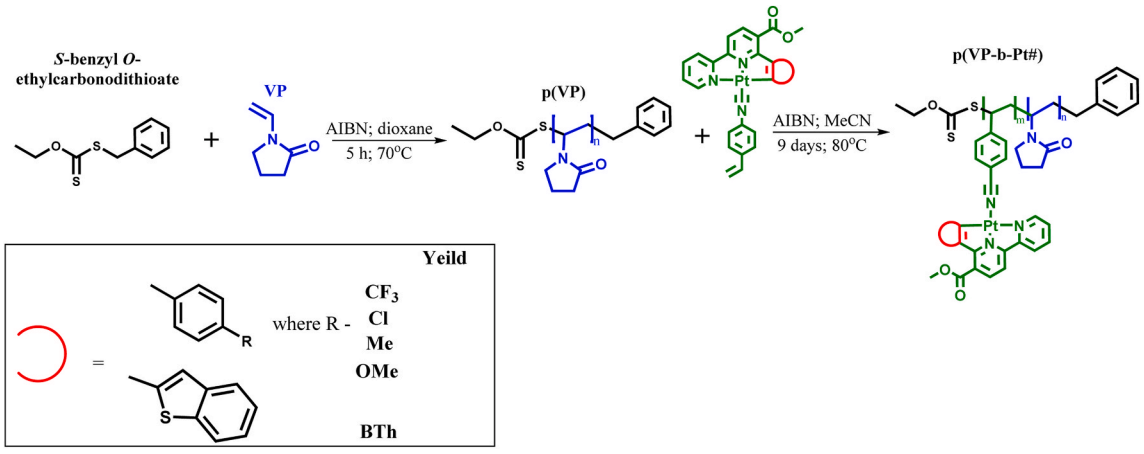

Scheme 2. Synthesis of **p(VP-*b*-Pt-#)** block-copolymers.

all but one complexes and size distribution is unimodal (Table 2, Fig. S13). We did not observe any peaks in the area of 7–12 nm characteristic for **p(VP)** [35] despite of impossibility to separate it from the copolymers. Therefore, it can be suggested that **p(VP)** plays the role of protective colloid localized in the shell of NPS and additionally stabilizes them [36]. The size of the NPS based on **p(VP-*b*-Pt-CF$_3$)** is substantially higher than those found for the other copolymers that can be explained by deviation of the NPS form from ball-like structure typical for classic micelles. Indeed, in all cases excluding **p(VP-b-Pt-CF$_3$)**, the TEM images displayed the NPS size comparable to that found in DLS measurements and ball-like structures (Fig. S14). Despite of the similar nature of complexes, the NPS based on **p(VP-b-Pt-CF$_3$)** shows significantly different appearance, which can be considered as worm-like aggregates of the micelles (Fig. S14A). Closely analogous behavior of copolymers containing platinum complexes with the same ligand was revealed earlier [25] that points to a particular feature of the ligand effect onto the structure of the corresponding NPS.

The copolymers luminesce in organic and aqueous solutions, their photophysical characteristics are given in Table 3, absorption, excitation and emission spectra are shown in Figs. S15 and 3, respectively.

First of all, it has to be noted that a low degree of copolymerization and impossibility of starting **p(VP)** and copolymer molecules separation strongly affect the emission spectra. Due to a low degree of copolymerization for all copolymers, excluding **p(VP-b-Pt-CF$_3$)**, one can observe domination of the **p(VP)** chain emission in the corresponding spectra. Nevertheless, some general features of platinum chromophores

Table 2
The characteristics of **p(VP-*b*-Pt-#)** in aqueous solution: molecular weight, particle size, polydispersity index, and average number of Pt units in the copolymers.

Copolymer	Molecular weight[a]				D (TEM), nm	D (DLS), nm	PDI (DLS)	Pt, units[c]
	M_n	M_w	Đ	M_{calc}[b]				
p(VP)	4650	8450	1.82					
p(VP-*b*-Pt-CF_3)	5300	9150	1.72	9180	200	162	0.248	1.90
p(VP-*b*-Pt-Cl)	5550	10300	1.86	9000	35	31	0.582	1.26
p(VP-*b*-Pt-Me)	5200	9850	1.89	9200	80	75	0.40	1.09
p(VP-*b*-Pt-OMe)	4600	8800	1.91	8500	45	61	0.478	0.42
p(VP-*b*-Pt-BTh)	5150	9200	1.66	8550	40	52	0.502	0.53

[a] M_n, M_w – the number and weight average molecular weights, respectively, obtained from GPC, Đ – the polydispersity coefficient equaled M_w/M_n.
[b] M_{calc} – the calculated molecular weight via ICP OES.
[c] average number of Pt complexes per macromolecule measured by ICP OES (more details in Table S1).

Table 3
Photophysical properties of copolymers in DCM and aqueous solutions. Excitation spectra and lifetimes were monitored at emission band maxima of platinum chromophores.

Copolymer	Solution	λ_{abs}, nm	λ_{exc}, nm	λ_{em},[a] nm	Φ_{aer}/Φ_{deg},[a] %	τ_{aer}/τ_{deg},[a] ns
p(VP-b-Pt-CF_3)	DCM	282, 328, 448sh	356, 558, 606	421, 570, 631	0.9/1.4	570/651
	H_2O	277sh, 413sh, 577sh	420sh, 554	770	0.06/0.06	[b]
p(VP-b-Pt-Cl)	DCM	282, 329, 430sh, 545sh	361sh, 446sh, 531	452, 604	1.3/1.3	232/270
	H_2O	272sh, 309sh, 419sh	416sh, 520sh	450, 768	<0.01/<0.01	[b]
p(VP-b-Pt-Me)	DCM	278sh, 345sh, 425sh	356, 442sh	436, 550	0.43/0.59	812/1073
	H_2O	278sh, 345sh, 425sh	421sh	446sh, 802	<0.01/<0.01	[b]
p(VP-b-Pt-OMe)	DCM	281, 343sh, 606	361, 558, 605	459, 637	0.7/1.7	291/523
	H_2O	297, 339sh	335sh, 435sh, 563	803	0.17/0.17	[b]
p(VP-b-Pt-BTh)	DCM	283, 476sh, 613sh	323, 435sh	493, 755	0.38/0.49	393/450
	H_2O	274sh, 384sh	280, 349sh, 478sh	511, 758	<0.01/<0.01	[b]

[a] $\lambda_{exc} = 365$ nm.
[b] Emission band is out of instrument working interval.

behavior in DCM and aqueous media can be formulated.

The emission characteristics of the copolymers in DCM and water are essentially different illustrating substantial variations in the conformational behavior of polymerized platinum chromophores in these media, which also depends on the nature of pincer ligands. In DCM solution, the four complexes containing substituted phenyl-bipyridine skeleton display broaden emission bands, each of which may be considered as a combination of emissions from isolated mononuclear platinum chromophores and their aggregated forms, see Fig. 3a–d. The short wavelength components of the broaden bands overlap with the emission bands of isolated platinum chromophores (complexes in DCM), whereas the long wavelength tails may be assigned to the contribution of emission from pairwise aggregated chromophores as they fits well the emission bands observed for the solid-state samples of the corresponding complexes, Fig. 3. These observations indicate that despite of the low average number of complex molecules per one polymeric chain (less than 1.0, see Table 2) the real number is higher than 2.0 that made possible formation of binary aggregates due to intramolecular interaction between adjacent molecules of the complexes in the hydrophobic fragments of polymeric chains.

In aqueous solution, the emission of this group of copolymers display strong red shift of emission bands (for ca. 150–200 nm) compared to those found for the copolymers in DCM. This observation indicates that in the micellar species formed in water the character of interaction between the chromophores has been changed from intramolecular coupling of the platinum centers to formation of intermolecular aggregates in a way similar to that observed earlier in closely analogous systems [21,25,28]. The stronger red shift in aqueous media compared to DCM solution may be explained either by stronger aggregation (shorter Pt–Pt contacts) of the chromophores due to more favorable configuration of the platinum centers in the intermolecular aggregates or because of multiple character of the aggregates in micelles. In contrast, the observed weak emission bands of **p(VP-b-Pt-BTh)** in DCM and in water are nearly identical and fit well emission of the **Pt–BTh** complex in DCM and in solid state. These data indicate that this particular chromophore does not exhibit any tendency toward aggregation neither in solid state nor in polymeric chains evidently due to specific way of π−π stacking of the ligand aromatic fragments [21], which does not allow effective Pt–Pt bonding.

3. Conclusion

In conclusion, a series of platinum NˆNˆC pincer complexes with isocyanide-styrene ligand in the fourth position was synthesized and their photophysics was studied in detail. In solution, the complexes display phosphorescence from ^{3}MLCT excited state demonstrating typical emission wavelength dependence on the donor properties of substituents in the NˆNˆC ligands and on the size their aromatic systems. In solid state, the observed emission bands for all but one complexes display a considerable red shift, which may be ascribed to formation of binary aggregates with short Pt–Pt contacts that change the character of emissive excited state to ^{3}MMLCT. The styrene function of the isocyanide ligand allows complexes copolymerizing with polyvinylpyrrolidone using RAFT chemistry to give amphiphilic block copolymers, which are soluble in organic solvents and water. The hydrophobic block of the copolymers consists of a few copolymerized platinum complexes, the photophysical behavior of which in organic and water solutions is dictated by a specific configuration of the mononuclear platinum fragments in the polymeric chain. In organic solvent, the copolymer exists as isolated molecular entities that makes possible only a limited (most probably binary) intramolecular aggregation of the platinum chromophores in a way similar to that observed in solid state. As a result, one can observe a mixed emission bands of the copolymers composed of phosphorescence from isolated platinum chromophores and binary aggregates from ^{3}ILCT/^{3}MLCT and ^{3}MMLCT, respectively. On the contrary, in aqueous media hydrophobicity of the platinum containing blocks provokes formation of micellar type

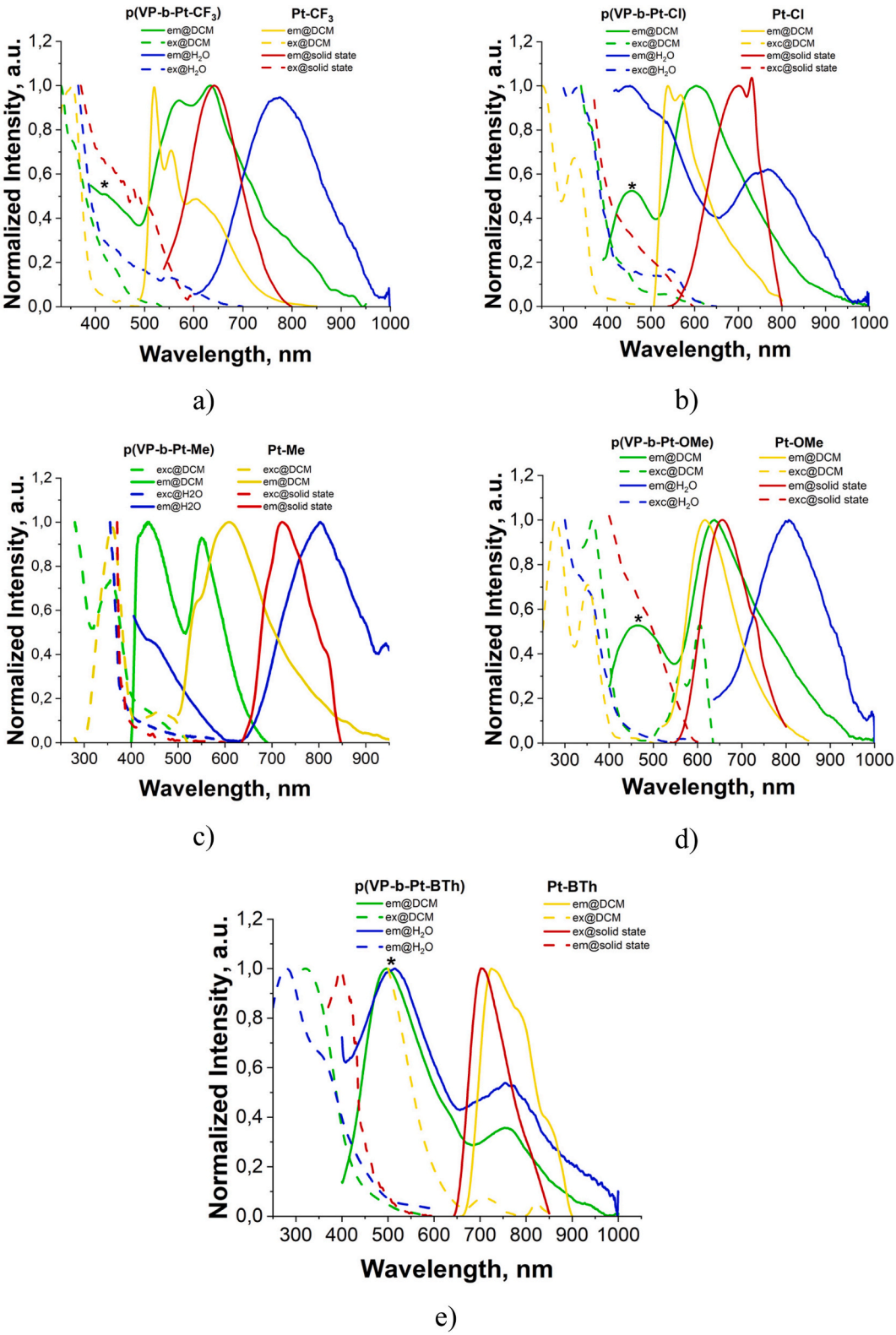

Fig. 3. Comparative excitation and emission spectra of Pt complexes in DCM, in solid state and **p(VP-b-Pt-#)** copolymers in DCM and aqueous solution. Emission spectra were obtained using excitation at 365 nm, excitation spectra were recorded at emission band maxima. Peaks marked with asterisk (*) are related to p(VP)emission.

nanospecies, where flexibility of the polymeric chains allows for intermolecular aggregating of the platinum chromophores with tighter contacts of the platinum centers and multiple character of the aggregates to give much stronger red shift of emission down to 803 nm in the case of **p(VP-b-Pt-OMe)**. It is also worth noting that solubility of the obtained copolymers in aqueous solutions makes possible their potential application in biological experiments as NIR emitting probes.

4. Experimental

All reagents and solvents were used as received unless otherwise specified. K_2PtCl_4, silver triflate, glacial acetic acid, methanol, diethyl ether, acetonitrile, dichloromethane, and deuterated solvents (dichloromethane-*d2*, DMSO-d_6, acetonitrile-*d3*) were obtained commercially. Dichloromethane for photophysical measurements was purified by sequential sulfuric acid (conc. H_2SO_4) washing, neutralization (sat. aq. NaCl), drying (Na_2SO_4), and refluxing over P_2O_5 prior to distillation.

N-vinylpyrrolidone and azobisisobutyronitrile (AIBN) were vacuum-distillated and recrystallized from ethanol at 50 °C, respectively. All the NNC ligands (**CF3** – methyl 6-(4-(trifluoromethyl)phenyl)-[2,2′-bipyridine]-5-carboxylate, **Cl** – methyl 6-(4-chlorophenyl)-[2,2′-bipyridine]-5-carboxylate, **Me** – methyl 6-(p-tolyl)-[2,2′-bipyridine]-5-carboxylate, **OMe** – methyl 6-(4-methoxyphenyl)-[2,2′-bipyridine]-5-carboxylate, **BTh** – methyl 6-(benzo[b]thiophen-2-yl)-[2,2′-bipyridine]-5-carboxylate) were synthesized according to published procedure [37].

5. General experimental details

Mass spectrometry analysis was performed using a Bruker maXis HRMS-ESI-QTOF mass spectrometer in positive electrospray ionization mode (ESI+). NMR spectra (^{1}H and ^{1}H–^{1}H COSY) were acquired on a Bruker Avance III spectrometer operating at 400 MHz. Chemical shifts for ^{1}H NMR spectra were referenced to residual proton signals of the deuterated solvents.

1-Isocyano-4-vinylbenzene was synthesized following a modified literature procedure starting from *N*-(4-vinylphenyl)formamide [38]. A solution of *N*-(4-vinylphenyl)formamide (2 g, 13.6 mmol) in anhydrous CH_2Cl_2 (50 mL) was cooled to −10 °C under an argon atmosphere. Triethylamine (5 g, 50 mmol) was added, followed by the dropwise addition of $POCl_3$ (2.3 g, 15 mmol), maintaining the reaction temperature below −10 °C. The reaction mixture was stirred at −10 °C for 2 h and then quenched by the addition of saturated sodium carbonate solution (40 mL). The mixture was allowed to warm to room temperature and stirred for an additional hour. The organic layer was separated, and the aqueous phase was further extracted with CH_2Cl_2 (3 × 30 mL). The combined organic extracts were dried over anhydrous sodium sulfate and concentrated under reduced pressure using a rotary evaporator. The crude product was purified by column chromatography (ethyl acetate/hexane, 1:5) to afford the desired isocyanide as a dark oil (0.9 g, 51 % yield). ^{1}H NMR (400 MHz, $CDCl_3$) δ 7.42 (d, 2H, J = 8.4 Hz), 7.35 (d, 2H, J = 8.4 Hz), 6.71 (dd, 1H, J = 17.6, 10.9 Hz), 5.80 (d, 1H, J = 17.6 Hz), 5.38 (d, 1H, J = 10.9 Hz). ^{13}C{^{1}H} NMR (100 MHz, $CDCl_3$) δ 164.59 (t, J = 5.5 Hz), 138.70, 135.27, 127.57, 127.06, 125.63 (t, J = 13.9 Hz), 116.36.

6. General procedure for the synthesis of Pt–CF_3 – Pt–BTh

At the first stage, the NˆNˆC ligand and K_2PtCl_4 were boiled in acetic acid for 24 h. The resulting sediment was sequentially washed with water, methanol, and diethyl ether. After drying, CF_3SO_3Ag was added and the resulting mixture was then boiled in acetonitrile for 2 h. To remove precipitated silver chloride the resulting solution was filtered through a pipette with cottonwool and a layer of celite (approximately 1 cm). The acetonitrile was evaporated with a rotary evaporator and the acetonitrile complex was dissolved in dichloromethane, followed by of addition of 4-vinylphenylisocyanide and catalyst (CuI). The resulting mixture was stirred for 3 h at 40 °C. After that the solution was filtered through a pipette filter to remove the catalyst, the solvent was removed using a rotary evaporator. The final products were recrystallized from dichloromethane-hexane solvent system.

Pt-CF3. Bright orange needles. 38 mg (Yield 62 %). ^{1}H NMR (400 MHz, Methylene Chloride-d_2) δ 9.00 (d, 1H), 8.50 (d, 1H), 8.44 (d, 1H), 8.28 (td, 1H), 8.23 (d, 1H), 7.96–7.88 (m, 1H), 7.75 (d, 2H), 7.70–7.61 (m, 2H), 7.59 (s, 1H), 7.45 (d, 1H), 7.40–7.33 (m, 1H), 6.83 (dd, 1H), 5.97 (d, 1H), 5.55 (d, 1H), 4.07 (s, 3H). HR-ESI/MS (*m/z*): calcd. for C29H23F3N3O3Pt [M + CH3OH]$^+$ 713.1338, found 713.1278.

Pt–Cl. Bright red cotton-like substance. 71 mg (Yield 57 %). ^{1}H NMR (400 MHz, DMSO-d_6) δ 8.87 (d, J = 4.6 Hz, 1H), 8.48 (d, J = 7.9 Hz, 1H), 8.34 (dd, J = 12.6, 7.8 Hz, 2H), 8.15 (t, J = 9.9 Hz, 1H), 7.99–7.72 (m, 6H), 7.40 (dt, J = 16.0, 7.4 Hz, 3H), 6.91 (dd, J = 17.5, 10.9 Hz, 1H), 6.08 (d, 1H), 5.55 (d, 1H), 4.05 (s, 3H). HR-ESI/MS (*m/z*): calcd. for C27H19ClN3O2Pt [M]$^+$ 648.0808, found 648.0797.

Pt–Me. Yellowish-brown prisms. 25 mg (Yield 50 %). ^{1}H NMR (400 MHz, DMSO-d_6) δ 8.95–8.84 (m, 1H), 8.38 (d, J = 8.3 Hz, 1H), 8.35–8.27 (m, 1H), 8.21 (d, J = 5.0 Hz, 2H), 7.84 (dd, J = 14.4, 7.3 Hz, 3H), 7.75 (d, J = 8.4 Hz, 2H), 6.94–6.74 (m, 4H), 6.08 (d, J = 17.7 Hz, 1H), 5.52 (d, J = 11.0 Hz, 1H), 3.98 (d, J = 10.7 Hz, 6H). HR-ESI/MS (*m/z*): calcd. for C28H23ClN3O2Pt [M + HCl]$^+$ 664.1127, found 664.1132.

Pt–OMe. Bright red cotton-like substance. 85 mg (Yield 70 %). ^{1}H NMR (400 MHz, DMSO-d_6) δ 9.01 (d, J = 4.9 Hz, 1H), 8.56 (d, 1H), 8.42 (t, J = 8.4 Hz, 1H), 8.29 (dd, J = 1.8 Hz, 2H), 7.87 (dd, J = 12.5, 7.6 Hz, 3H), 7.75 (d, J = 8.5 Hz, 2H), 7.20 (d, J = 8.8 Hz, 1H), 6.96–6.85 (m, 1H), 6.83 (d, J = 2.7 Hz, 1H), 6.72 (dd, J = 8.9, 2.5 Hz, 1H), 6.06 (d, J = 17.7 Hz, 1H), 5.52 (d, J = 11.0 Hz, 1H), 3.99 (s, 3H), 3.77 (s, 3H). HR-ESI/MS (*m/z*): calcd. for C28H22N3O3Pt [M]$^+$ 643.1308, found 643.1297.

Pt–BTh. Brown needles. ^{1}H NMR (400 MHz, Acetonitrile-d_3) δ 8.28 (d, 1H), 7.96 (t, 2H), 7.81 (d, 1H), 7.59 (d, 2H), 7.56–7.40 (m, 6H), 7.27 (t, 2H), 6.86 (dd, 1H), 6.02 (d, 1H), 5.57 (d, 1H), 3.92 (s, 3H). HR-ESI/MS (*m/z*): calcd. For C29H22N3O2PtS [C29H22N3O2PtS]$^+$ 671.1080, found 671.1070.

7. Synthesis of macro-RAFT agent

p(VP) as a macro-RAFT agent for obtaining phosphorescent block copolymers was synthesized as described earlier [25,28,29] with slight modification of the procedure to vary the polymer molecular weight. N-vinylpyrrolidone (22 mmol) and azobisisobutyronitrile (AIBN, 20 μmol) were dissolved in 9 mL of freshly distilled dioxane. The RAFT agent, *S*,*S*-dibenzyltrithiocarbonate (45 mmol), was simultaneously dissolved in 1 mL of dioxane and then added to the reaction mixture. The obtained solution was degassed by three repeated freeze−pump−thaw cycles and sealed. The reaction was left at 70 °C under vigorous stirring for 5 h. The product (macro-RAFT agent) was purified by dialysis (MWCO 3500), reaction yield ca. 30 %.

^{1}H NMR (400 MHz, D_2O, δ): 7.58–7.40 (d, 5H), 4.12–3.67 (d, 92H), 3.67–3.28 (s, 185H), 2.74–2.38 (m, 197H), 2.38–2.12 (s, 191H), 2.12–1.72 (d, 191H).

8. Block copolymer synthesis

16 mg of **p(VP)** (1.16 μmol), **AIBN** (0.116 μmol), and a 4-fold of excess of isocyanide platinum complexes (see Scheme 2, 4.64 μmol for each complex) were dissolved in 10 mL of acetonitrile. The reaction mixture was then degassed by three repeated freeze−pump−thaw cycles and sealed, heated to 80 °C and left under vigorous stirring for 48 h. The same amount of AIBN was also added twice into the reaction mixture in each 72 h until the solutions afford colored precipitates. The solvent was removed using rotary evaporator, the precipitate was dissolved in water, centrifuged 3 times and then dialyzed for 2 days (Molecular weight cut-off = 3500) followed by lyophilization. The copolymer mass measured gravimetrically varied from 58 to 90 wt% relative to the amount of starting reagents.

9. Characterization of polymers

Hydrodynamic diameters were measured in water by Dynamic Light Scattering using Malvern ZetaSizer NanoZS and were calculated as

average of three individual measurements.

Chromatographic analysis was performed on a Shimadzu LC-20AD chromatograph equipped with the refractive detector. Samples were studied with Waters Styragel HT4 column (10 μm, 7.8 × 300 mm). A LiCl solution (5 mmol/l) in DMF at a temperature of 60 °C was used as the mobile phase. Polyethylene oxide standards were chosen for calibration curve.

The amount of Pt units in copolymers was determined by Inductively Coupled Plasma Optical Emission Spectroscopy (ICPE-9000, Shimadzu). Platinum was detected at 203.646 and 214.423 nm. The water-soluble complex [(methyl 2-phenylquinoline-carboxylate)Pt (1,2-bis(diphenylphosphino)benzene-SO_3Na] was used as a standard for calibration [39].

10. Photophysical measurements

UV–Vis absorption spectra were recorded for dichloromethane solutions using a Shimadzu UV-1800 spectrophotometer. Emission spectra were acquired on an Avantes AvaSpec-2048x64 spectrometer under 365 nm LED excitation. Excitation spectra were measured using a Shimadzu UV-2550 spectrophotometer.

Emission quantum yields (Φ) were determined via the comparative method, with Ru (bpy)$_3$ [PF$_6$]$_2$ aerated water solution ($\Phi_{ref} = 0.042$) [40] as the reference, following the established equation [41]:

$$\Phi_s = \Phi_r \frac{n_s^2 A_r I_s}{n_r^2 A_s I_r}$$

The quantum yield (Φ_s) of the sample was determined relative to a reference compound (Φ_r), correcting for the solvent refractive index (η) ($\eta(H_2O) = 1.333$, $\eta(CH_2Cl_2) = 1.424$). The absorbances of the sample (A_s) and reference (A_r) were measured at the excitation wavelength, and the integrated phosphorescence intensities (I_s and I_r) were obtained from the corresponding emission bands.

For solid-state samples, quantum yield measurements were performed on a Fluorolog-3 spectrofluorometer (HORIBA Jobin Yvon) equipped with an integrating sphere (Quanta-phi). Excitation spectra were recorded using the same spectrofluorometer.

Excited-state lifetimes were measured via time-correlated single-photon counting (TCSPC) using a pulsed DTL-375QT laser (355 nm, 1 kHz repetition rate) as the excitation source. The detection system consisted of a Tektronix DPO2012B oscilloscope (100 MHz bandwidth), Ocean Optics Monoscan-2000 monochromator (1 nm resolution), FASTComTec MCS6A1T4 time digitizer, and Hamamatsu H10682-01 photomultiplier tube. Emission decay curves were processed using Origin 9.0 software with monoexponential fitting to extract lifetime components.

CRediT authorship contribution statement

Elizaveta V. Durova: Data curation, Investigation, Visualization. **Rostislav R. Shulepov:** Investigation. **Vadim A. Baigildin:** Formal analysis, Investigation, Methodology, Writing – original draft. **Mikhail A. Kinzhalov:** Conceptualization, Investigation. **Mikhail P. Kurlykin:** Investigation, Resources. **Viktor V. Sokolov:** Investigation, Methodology. **Sergey P. Tunik:** Writing – original draft.

Funding

In commemoration of the 300th anniversary of St Petersburg State University's founding. This study was funded by the Russian Science Foundation, grant No. 24-13-00084.

Declaration of competing interest

The authors declare that they have no known competing financial interests or personal relationships that could have appeared to influence the work reported in this paper.

Acknowledgments

The work was performed using the equipment of the Research Park of St. Petersburg State University: Centers for Magnetic Resonance, for Chemical Analysis and Materials Research, for X-ray Diffraction Studies, for Optical and Laser Materials Research, Cryogenic department, and Nanotechnology.

Appendix A. Supplementary data

Supplementary data to this article can be found online at https://doi.org/10.1016/j.omx.2025.100425.

Data availability

Data will be made available on request.

References

[1] V.P. Boyarskiy, N.A. Bokach, K.V. Luzyanin, V.Y. Kukushkin, Metal-mediated and metal-catalyzed reactions of isocyanides, Chem. Rev. 115 (2015) 2698–2779. https://doi.org/10.1021/cr500380d.
[2] M.A. Kinzhalov, K.V. Luzyanin, Synthesis and contemporary applications of Platinum group metals complexes with acyclic diaminocarbene ligands, Russ. J. Inorg. Chem. 67 (2022) 48–90. https://doi.org/10.1134/S0036023622010065.
[3] M.V. Kashina, K.V. Luzyanin, E.A. Katlenok, M.A. Kinzhalov, Green-light hydrosilylation photocatalysis with Platinum(II)Metalla-N-Heterocyclic carbene complexes, Chem. Eur J. 30 (2024) e202403264. https://doi.org/10.1002/chem.202403264.
[4] A.I. Solomatina, I.O. Aleksandrova, A.J. Karttunen, S.P. Tunik, I.O. Koshevoy, Dibenzothiophene-platinated complexes: probing the effect of ancillary ligands on the photophysical performance, Dalton Trans. 46 (2017) 3895–3905. https://doi.org/10.1039/C7DT00349H.
[5] E.V. Sokolova, M.A. Kinzhalov, A.S. Smirnov, A.M. Cheranyova, D.M. Ivanov, V. Y. Kukushkin, N.A. Bokach, Polymorph-dependent phosphorescence of cyclometalated Platinum(II) complexes and its relation to non-covalent interactions, ACS Omega. 7 (2022) 34454–34462. https://doi.org/10.1021/acsomega.2c04110.
[6] M. Martínez-Junquera, R. Lara, E. Lalinde, M.T. Moreno, Isomerism, aggregation-induced emission and mechanochromism of isocyanide cycloplatinated(II) complexes, J. Mater. Chem. C. 8 (2020) 7221–7233, https://doi.org/10.1039/D0TC01163K.
[7] G.D. Sutton, M.E. Olumba, Y.H. Nguyen, T.S. Teets, The diverse functions of isocyanides in phosphorescent metal complexes, Dalton Trans 50 (2021) 17851–17863. https://doi.org/10.1039/D1DT03312C.
[8] J. Sanning, L. Stegemann, P.R. Ewen, C. Schwermann, C.G. Daniliuc, D. Zhang, N. Lin, L. Duan, D. Wegner, N.L. Doltsinis, C.A. Strassert, Colour-tunable asymmetric cyclometalated Pt(II) complexes and STM-assisted stability assessment of ancillary ligands for OLEDs, J. Mater. Chem. C. 4 (2016) 2560–2565. https://doi.org/10.1039/C6TC00093B.
[9] S.A. Katkova, D.O. Kozina, K.S. Kisel, M.A. Sandzhieva, D.A. Tarvanen, S. V. Makarov, V.V. Porsev, S.P. Tunik, M.A. Kinzhalov, Cyclometalated platinum(II) complexes with acyclic diaminocarbene ligands for OLED application, Dalton Trans. 52 (2023) 4595–4605. https://doi.org/10.1039/D3DT00080J.
[10] Y.H. Nguyen, L.T.M. Dang, M. Cornu, C. Jiang, A.C. Darrow, V.Q. Dang, T.S. Teets, Luminescent cyclometalated platinum acyclic diaminocarbene complexes as PhOLED dopants, ACS Appl. Opt. Mater. 2 (2024) 2019–2030. https://doi.org/10.1021/acsaom.4c00347.
[11] R.W.-Y. Sun, A.L.-F. Chow, X.-H. Li, J.J. Yan, St. S.-Y. Chui, C.-M. Che, Luminescent cyclometalated platinum(II) complexes containing N-heterocyclic carbene ligands with potent in vitro and in vivo anti-cancer properties accumulate in cytoplasmic structures of cancer cells, Chem. Sci. 2 (2011) 728–736. https://doi.org/10.1039/C0SC00593B.
[12] M. Yuen, V.A.L. Roy, W. Lu, S.C.F. Kui, G.S.M. Tong, M. So, S.S. Chui, M. Muccini, J.Q. Ning, S.J. Xu, C. Che, Semiconducting and electroluminescent nanowires self-assembled from Organoplatinum(II) complexes, Angew. Chem. Int. Ed. 47 (2008) 9895–9899. https://doi.org/10.1002/anie.200802981.
[13] W. Lu, Y. Chen, V.A.L. Roy, S.S. Chui, C. Che, Supramolecular polymers and chromonic mesophases self-organized from phosphorescent cationic Organoplatinum(II) complexes in water, Angew. Chem. Int. Ed. 48 (2009) 7621–7625. https://doi.org/10.1002/anie.200903109.
[14] J.L.-L. Tsai, T. Zou, J. Liu, T. Chen, A.O.-Y. Chan, C. Yang, C.-N. Lok, C.-M. Che, Luminescent platinum(II) complexes with self-assembly and anti-cancer properties: hydrogel, pH dependent emission color and sustained-release properties under physiological conditions, Chem. Sci. 6 (2015) 3823–3830. https://doi.org/10.1039/C4SC03635B.
[15] Q. Wan, D. Li, J. Zou, T. Yan, R. Zhu, K. Xiao, S. Yue, X. Cui, Y. Weng, C. Che, Efficient long-range triplet exciton transport by metal–metal interaction at room

temperature, Angew. Chem. Int. Ed. 61 (2022) e202114323. https://doi.org/10.1002/anie.202114323.
[16] J. Chen, L. Ao, C. Wei, C. Wang, F. Wang, Self-assembly of platinum(ii) 6-phenyl-2,2′-bipyridine complexes with solvato- and iono-chromic phenomena, Chem. Commun. 55 (2019) 229–232. https://doi.org/10.1039/C8CC06770H.
[17] M. Liu, Y. Han, H. Zhong, X. Zhang, F. Wang, Supramolecular chirogenesis induced by Platinum(II) tweezers with excellent environmental tolerance, Angew. Chem. Int. Ed. 60 (2021) 3498–3503. https://doi.org/10.1002/anie.202012901.
[18] Z. Li, Y. Han, F. Nie, M. Liu, H. Zhong, F. Wang, Bright and robust phosphorescence achieved by non-covalent clipping, Angew. Chem. Int. Ed. 60 (2021) 8212–8219. https://doi.org/10.1002/anie.202015846.
[19] Q. Wan, D. Li, J. Zou, T. Yan, R. Zhu, K. Xiao, S. Yue, X. Cui, Y. Weng, C. Che, Efficient long-range triplet exciton transport by metal–metal interaction at room temperature, Angew. Chem. 134 (2022) e202114323. https://doi.org/10.1002/ange.202114323.
[20] Y. Chen, C.-M. Che, W. Lu, Phosphorescent organoplatinum(ii) complexes with a lipophilic anion: supramolecular soft nanomaterials through ionic self-assembly and metallophilicity, Chem. Commun. 51 (2015) 5371–5374. https://doi.org/10.1039/C4CC08569H.
[21] E.V. Durova, E.E. Galenko, A.A. Shtyrov, M.N. Ryazantsev, K.S. Kisel, J. R. Shakirova, S.P. Tunik, A new family of Pt(II) isocyanide complexes with NNC-type pincer ligands: correlation between structural features and aggregation-induced emission, Opt. Mater. 162 (2025) 116926. https://doi.org/10.1016/j.optmat.2025.116926.
[22] T. Moriuchi, Y. Sakamoto, S. Noguchi, T. Fujiwara, S. Akine, T. Nabeshima, T. Hirao, Design and controlled emission properties of bioorganometallic compounds composed of uracils and organoplatinum(ii) moieties, Dalton Trans. 41 (2012) 8524–8531. https://doi.org/10.1039/c2dt30533j.
[23] M. Martínez-Junquera, E. Lalinde, M.T. Moreno, Multistimuli-Responsive properties of aggregated Isocyanide Cycloplatinated(II) complexes, Inorg. Chem. 61 (2022) 10898–10914. https://doi.org/10.1021/acs.inorgchem.2c01400.
[24] T. Theiss, S. Buss, I. Maisuls, R. López-Arteaga, D. Brünink, J. Kösters, A. Hepp, N. L. Doltsinis, E.A. Weiss, C.A. Strassert, Room-temperature phosphorescence from Pd(II) and Pt(II) complexes as supramolecular luminophores: the role of self-assembly, metal–metal interactions, spin–orbit coupling, and ligand-field splitting, J. Am. Chem. Soc. 145 (2023) 3937–3951. https://doi.org/10.1021/jacs.2c09775.
[25] M. Samandarsangari, R.R. Shulepov, V.A. Baigildin, J.R. Shakirova, V.V. Sokolov, E.V. Durova, D.M. Nikolaev, M.N. Ryazantsev, K.S. Kisel, S.P. Tunik, Synthesis, characterization, and photophysical properties of water-soluble AIE chromophores based on alkynyl-styrene Pt(II) pincer complexes conjugated with polyvinylpyrrolidone using RAFT polymerization, Inorg. Chem. 64 (2025) 12742–12754. https://doi.org/10.1021/acs.inorgchem.5c01567.
[26] J.V. Caspar, E.M. Kober, B.P. Sullivan, T.J. Meyer, Application of the energy gap law to the decay of charge-transfer excited states, J. Am. Chem. Soc. 104 (1982) 630–632. https://doi.org/10.1021/ja00366a051.
[27] J.V. Caspar, T.J. Meyer, Application of the energy gap law to nonradiative, excited-state decay, J. Phys. Chem. 87 (1983) 952–957. https://doi.org/10.1021/j100229a010.
[28] R.A. Shilov, V.A. Baigildin, K.S. Kisel, E.E. Galenko, A.S. Gubarev, M.E. Mikhailova, O.S. Vezo, N.V. Tsvetkov, A.A. Shtyrov, M.N. Ryazantsev, J.R. Shakirova, S. P. Tunik, RAFT copolymerization of Pt(II) pincer complexes with water-soluble polymer as an efficient way to obtain micellar-type nanoparticles with aggregation-induced NIR emission, Aggregate 6 (2025) e713. https://doi.org/10.1002/agt2.713.
[29] R.A. Shilov, V.A. Baigildin, J.R. Shakirova, E.E. Galenko, E.V. Durova, S.P. Tunik, Synthesis, characterization and pH-sensitivity of AIE emitters obtained by RAFT polymerization of Pt(II) pincer complexes with polyvinylpyrrolidon, Opt. Mater. 157 (2024) 116317. https://doi.org/10.1016/j.optmat.2024.116317.
[30] C. Liu, C.-Y. Hong, C.-Y. Pan, Polymerization techniques in polymerization-induced self-assembly (PISA), Polym. Chem. 11 (2020) 3673–3689. https://doi.org/10.1039/D0PY00455C.
[31] W. Cai, W. Wan, C. Hong, C. Huang, C. Pan, Morphology transitions in RAFT polymerization, Soft Matter. 6 (2010) 5554–5561. https://doi.org/10.1039/c0sm00284d.
[32] J.-T. Sun, C.-Y. Hong, C.-Y. Pan, Recent advances in RAFT dispersion polymerization for preparation of block copolymer aggregates, Polym. Chem. 4 (2013) 873–881. https://doi.org/10.1039/C2PY20612A.
[33] Y. Zhang, G. Han, M. Cao, T. Guo, W. Zhang, Influence of solvophilic homopolymers on RAFT polymerization-induced self-assembly, Macromolecules 51 (2018) 4397–4406. https://doi.org/10.1021/acs.macromol.8b00690.
[34] D. Li, M. Huo, L. Liu, M. Zeng, X. Chen, X. Wang, J. Yuan, Overcoming kinetic trapping for morphology evolution during polymerization-induced self-assembly, Macromol. Rapid Commun. 40 (2019) 1900202. https://doi.org/10.1002/marc.201900202.
[35] G. Song, Y. Lin, Z. Zhu, H. Zheng, J. Qiao, C. He, H. Wang, Strong fluorescence of poly(N -vinylpyrrolidone) and its oxidized hydrolyzate, Macromol. Rapid Commun. 36 (2015) 278–285. https://doi.org/10.1002/marc.201400516.
[36] A. Bijlard, S. Wald, D. Crespy, A. Taden, F.R. Wurm, K. Landfester, Functional colloidal stabilization, Adv. Mater. Interfac. 4 (2017) 1600443. https://doi.org/10.1002/admi.201600443.
[37] E.E. Galenko, M.A. Kryukova, M.S. Novikov, A.F. Khlebnikov, Synthesis of Bi-, Ter-, and quaterpyridinecarboxylates via Propargylisoxazole–Pyridine rearrangement, J. Org. Chem. 85 (2020) 6109–6122. https://doi.org/10.1021/acs.joc.0c00611.
[38] M.A. Kinzhalov, M.V. Kashina, A.S. Mikherdov, E.A. Mozheeva, A.S. Novikov, A. S. Smirnov, D.M. Ivanov, M.A. Kryukova, A.Y. Ivanov, S.N. Smirnov, V. Y. Kukushkin, K.V. Luzyanin, Dramatically enhanced solubility of halide-containing organometallic species in diiodomethane: the role of solvent···Complex Halogen Bonding, Angew. Chem. Int. Ed. 57 (2018) 12785–12789. https://doi.org/10.1002/anie.201807642.
[39] A.I. Solomatina, S.-H. Su, M.M. Lukina, V.V. Dudenkova, V.I. Shcheslavskiy, C.-H. Wu, P.S. Chelushkin, P.-T. Chou, I.O. Koshevoy, S.P. Tunik, Water-soluble cyclometalated platinum(ii) and iridium(iii) complexes: synthesis, tuning of the photophysical properties, and *in vitro* and *in vivo* phosphorescence lifetime imaging, RSC Adv. 8 (2018) 17224–17236. https://doi.org/10.1039/C8RA02742K.
[40] K. Suzuki, A. Kobayashi, S. Kaneko, K. Takehira, T. Yoshihara, H. Ishida, Y. Shiina, S. Oishi, S. Tobita, Reevaluation of absolute luminescence quantum yields of standard solutions using a spectrometer with an integrating sphere and a back-thinned CCD detector, Phys. Chem. Chem. Phys. 11 (2009) 9850–9860. https://doi.org/10.1039/b912178a.
[41] A.T.R. Williams, S.A. Winfield, J.N. Miller, Relative fluorescence quantum yields using a computer-controlled luminescence spectrometer, Analyst 108 (1983) 1067–1071. https://doi.org/10.1039/an9830801067.